# Moon Shadow Observation by IceCube

**D.J. Boersma**[*], **L. Gladstone**[†] **and A. Karle**[†]
**for the IceCube Collaboration**[‡]

[*]*RWTH Aachen University, Germany*
[†]*Department of Physics, University of Wisconsin, Madison, WI 53706, USA*
[‡]*see special section of these proceedings*

*Abstract*. In the absence of an astrophysical standard candle, IceCube can study the deficit of cosmic rays from the direction of the Moon. The observation of this "Moon shadow" in the downgoing muon flux is an experimental verification of the absolute pointing accuracy and the angular resolution of the detector with respect to energetic muons passing through. The Moon shadow has been observed in the 40-string configuration of IceCube. This is the first stage of IceCube in which a Moon shadow analysis has been successful. Method, results, and some systematic error studies will be discussed.

*Keywords*: IceCube, Moon shadow, pointing capability

## I. INTRODUCTION

IceCube is a kilometer-cube scale Cherenkov detector at the geographical South Pole, designed to search for muons from high energy neutrino interactions. The arrival directions and energy information of these muons can be used to search for point sources of astrophysical neutrinos, one of the primary goals of IceCube.

The main component of IceCube is an array of optical sensors deployed in the glacial ice at depths between 1450 m and 2450 m. These Digital Optical Modules (DOMs), each containing a 25 cm diameter photomultiplier tube with accompanying electronics within a pressure housing, are lowered into the ice along "strings." There are currently 59 strings deployed of 86 planned; the data analyzed here were taken in a 40 string configuration, which was in operation between April 2008 and April 2009. There are 13 lunar months of data within that time. In this analysis we present results from 8 lunar months of the 40 string configuration.

For a muon with energy on the order of a TeV, IceCube can reconstruct an arrival direction with order 1° accuracy. For down-going directions, the vast majority of the detected muons do not originate from neutrino interactions, but from high energy cosmic ray interactions in the atmosphere. These cosmic ray muons are the dominant background in the search for astrophysical neutrinos. They can also be used to study the performance of our detector. In particular, we can verify the pointing capability by studying the shadow of the Moon in cosmic ray muons.

As the Earth travels through the interstellar medium, the Moon blocks some cosmic rays from reaching the Earth. Thus, when other cosmic rays shower in the Earth's atmosphere and create muons, there is a relative deficit of muons from the direction of the Moon. IceCube detects these muons, not the primary cosmic rays. Since the position and size of the Moon is so well known, the resulting deficit can be used for detector calibration. The idea of a Moon shadow was first proposed in 1957 [1], and has become an established observation for a number of astroparticle physics experiments; some examples are given in references [2], [3], [4], [5]. Experiments have used the Moon shadow to calibrate detector angular resolution and pointing accuracy [6]. They have also observed the shift of the Moon shadow due to the Earth's magnetic field [7]. The analysis described here is optimized for a first observation, and does not yet include detailed studies such as describing the shape of the observed deficit. These will be addressed in future studies.

## II. METHOD

### A. Data and online event selection

Data transfer from the South Pole is limited by the bandwidth of two satellites; thus, not all downgoing muon events can be immediately transmitted. This analysis uses a dedicated online event selection, choosing events with a minimum quality and a reconstructed direction within a window of acceptance around the direction of the Moon. The reconstruction used for the online event selection is a single (i.e., not iterated) log-likelihood fit.

The online event selection is defined as follows, where $\delta$ denotes the Moon declination:

- The Moon must be at least 15° above the horizon.
- At least 12 DOMs must register each event.
- At least 3 strings must contain hit DOMs.
- The reconstructed direction must be within 10° of the Moon in declination.
- The reconstructed direction must be within $40°/\cos(\delta)$ of the Moon in right ascension; the $\cos(\delta)$ factor corrects for projection effects.

These events are then sent via satellite to the northern hemisphere for further processing, including running the higher-quality 32-iteration log-likelihood reconstruction used in further analysis.

The Moon reached a maximum altitude of 27° above the horizon ($\delta = -27°$) in 2008, when viewed from
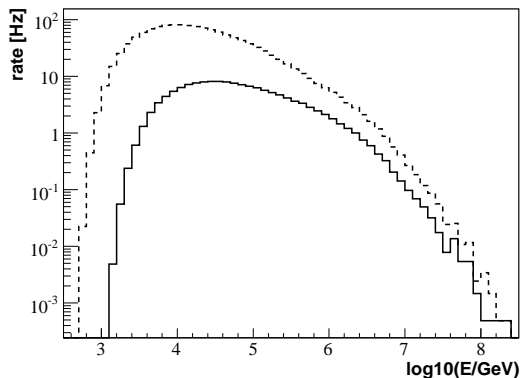
Fig. 1. The energy spectrum of (simulated) CR primaries of muons (or muon bundles) triggering IceCube. Dashed: all events; solid: primaries with $\delta > -30°$.
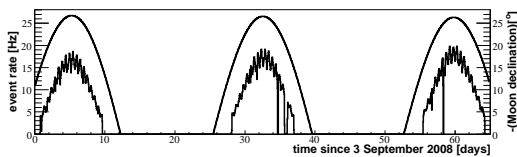


Fig. 2. The rate of events passing the Moon filter (in Hz, lower curve) averaged hourly, together with the position of the Moon above the horizon at the South Pole (in degrees, upper curve), plotted versus time over 3 typical months.

the IceCube detector. The trigger rate from cosmic ray muons is more than 1.2 kHz in the 40 string configuration, but most of those muons travel nearly vertically, and thus they cannot have come from directions near the Moon. Only $\sim 11\%$ of all muons that trigger the detector come from angles less than $30°$ above the horizon. Furthermore, muons which are closer to horizontal (and thus closer to the Moon) must travel farther before reaching the detector. They need a minimum energy to reach this far (see Fig. 1): the cosmic ray primaries which produce them must have energies of at least 2 TeV.

Three typical months of data are shown in Fig. 2, along with the position of the Moon above the horizon. The dominant shape is from the strong increase in muon flux with increasing angle above the horizon: as the Moon rises, so do the event rates near the Moon. This can be seen clearly in the correlation between the two sets of curves. There is a secondary effect from the layout of the 40 strings. One dimension of the detector layout has the full width (approximately 1km) of the completed detector, while the other is only about half as long. When the Moon is aligned with the short axis, fewer events pass the filter requirements. This causes the 12 hour modulation in the rate.

### B. Optimization of offline event selection and search bin size

A simulated data sample of $10^5$ downgoing muon events was generated using CORSIKA [8].

A set of cuts was developed using the following estimated relation between the significance $S$, the efficiency
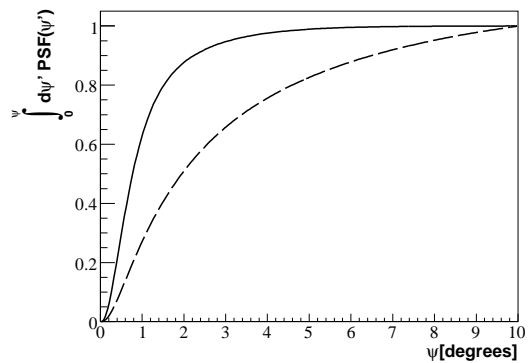


Fig. 3. The x-axis shows the angular difference $\psi$ between the true and reconstructed track. The y-axis shows the fraction of events with this or lower angular error. The solid curve shows the event sample after offline event selection, and the dashed curve shows the event sample after online event selection.

$\eta$ of events passing the cut, and the resulting median angular resolution $\Psi_{\mathrm{med}}$ of the sample:

$$S(\mathrm{cuts}) \propto \frac{\sqrt{\eta(\mathrm{cuts})}}{\Psi_{\mathrm{med}}(\mathrm{cuts})} \quad (1)$$

Since the deficit is based on high statistics of events in the search bin, this function provides a good estimator for optimizing the significance.

The following cuts were chosen:

- At least 6 DOMs are hit with light that hasn't been scattered in the ice, allowing a -15 nsec to +75 nsec window from some minimal scattering.
- Projected onto the reconstructed track, two of those hits at least 400 meters apart.
- The $1\sigma$ estimated error ellipse on the reconstructed direction has a mean radius less than $1.3°$.

The cumulative point spread function of the sample after the above quality cuts is shown as the solid black line in Fig. 3.

The size $\Psi_{\mathrm{search}}$ of the search bin is optimized for a maximally significant observation using a similar $\sqrt{N}$-error based argument and the resulting relation, which follows. Using the cumulative point spread function of the sample after quality cuts, we have:

$$S(\Psi_{\mathrm{search}}) \propto \frac{\int_0^{\Psi_{\mathrm{search}}} PSF(\psi')d\psi'}{\Psi_{\mathrm{search}}} \quad (2)$$

Maximizing this significance estimator gives an optimal search bin radius of $0.7°$. This analysis uses square bins with an area equal to that of the optimized round bin, with side length $1.25°$.

### C. Calculating significance

To show that the data are stable in right ascension $\alpha$, we show, in Fig. 4, the number of events in the central declination band. The errors shown are $\sqrt{N}$. The average of all bins excluding the Moon bin is 27747, which is plotted as a line to guide the eye. The Moon bin has 852
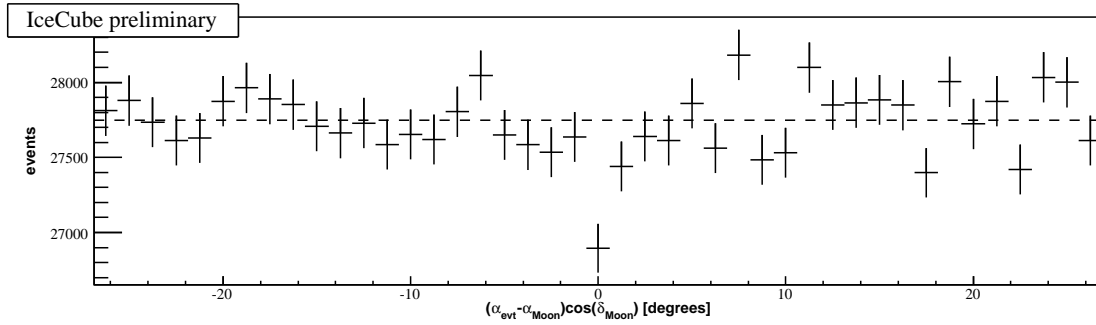
Fig. 4.　Number of events per 1.25° square bin, relative to the position of the Moon. The declination of the reconstructed track is within 0.625° bin from the declination of the Moon. The average of all bins except the Moon bin is shown as a dashedline to guide the eye.
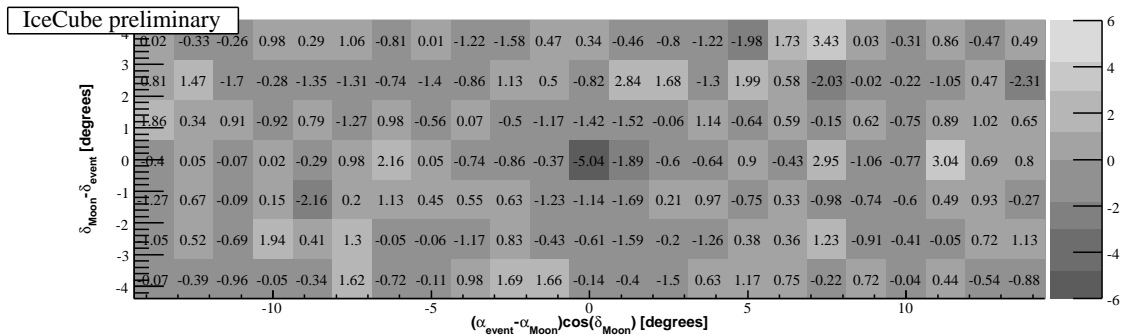


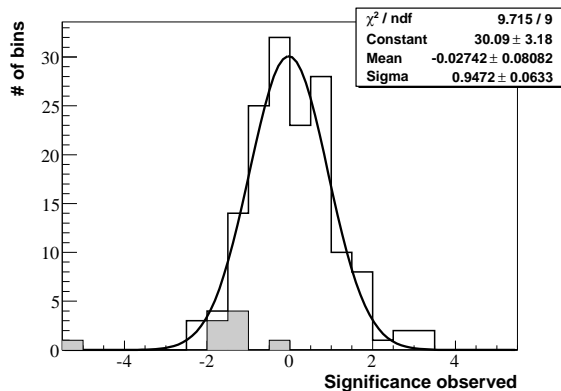Fig. 5.　The significance of deviations in a region centered on the Moon.



Fig. 6.　Each of the deviations shown in Fig. 5 is plotted here. The deviations of the central 9 bins are shown in gray. The surrounding bins are shown with a solid line histogram, and fit with a Gaussian curve.

events below this simple null estimate. This represents a 5.2σ deficit using $\sqrt{N}$ errors.

Although this shows that the data are stable, this error system is vulnerable to variations in small data samples. Although we don't see such variations here, we considered it prudent to consider an error system which takes into account the size of the background sample.

We used a standard formula from Li and Ma [9] for calculating the significance of a point source:

$$S = \frac{N_{\mathrm{on}} - \alpha N_{\mathrm{off}}}{\sqrt{\alpha(N_{\mathrm{on}} + N_{\mathrm{off}})}}. \qquad (3)$$

where $N_{\mathrm{on}}$ is the number of events in the signal sample, $N_{\mathrm{off}}$ is the number of events in the off-source region, and $\alpha$ is the ratio between observing times on- to off-source. We take $\alpha$ instead as the ratio of on- to off-source areas observed, since the times are equal.

The above significance formula is applied to the Moon data sample in the following way. The data are first plotted in the standard Moon-centered equatorial coordinates, correcting for projection effects with a factor of $\cos(\delta)$. The plot is binned using the $1.25° \times 1.25°$ bin size optimized in the simulation study. Each bin successively is considered as an on-source region. There is a very strong declination dependence in the downgoing muon flux, so variations of the order of the Moon deficit are only detectable in right ascension. Thus, off-source regions are selected within the same zenith band as the on-source region. Twenty off-source bins are used for each calculation: ten to the right and ten to the left of the on-source region, starting at the third bin out from the on-source bin (i.e., skipping two bins in between).

### III. RESULTS

For a region of 7 bins or $8.75°$ in declination $\delta$ and 23 bins or $28.75°$ in right ascension $\alpha$ around the Moon, the significance of the deviation of the count rate in each bin with respect to its off-source region was calculated, as described in section II-C. The result is plotted in Fig. 5. The Moon can be seen as the $5.0σ$ deficit in the central bin, at $(0,0)$.

To test the hypothesis that the fluctuations in the back-

ground away from the Moon are distributed randomly around 0, we plot them in Fig. 6. The central 9 bins, including the Moon bin, are not included in the Gaussian fit, but are plotted as the lower, shaded histogram. The width of the Gaussian fit is consistent with 1; therefore, the background is consistent with random fluctuations.

## IV. CONCLUSIONS AND FUTURE PLANS

IceCube has observed the shadow of the Moon as a $5.0\sigma$ deviation from event counts in nearby regions, using data from 8 of the total 13 lunar months in the data taking period with the 40-string detector setup. From this, we can conclude that IceCube has no systematic pointing error larger than the search bin, $1.25°$.

In the future, this analysis will be extended in many ways. First, we will include all data from the 40 string detector configuration. We hope to repeat this analysis using unbinned likelihood methods, and to describe the size, shape, and any offset of the Moon Shadow. We will then use the results of these studies to comment in more detail on the angular resolution of various reconstruction algorithms within IceCube. This analysis is one of the only end-to-end checks of IceCube systematics based only on experimental data.

## REFERENCES

[1] G.W. Clark, *Arrival Directions of Cosmic-Ray Air Showers from the Northern Sky* October 15, 1957, Physical Review Vol 108, no 2.

[2] A. Karle for the HEGRA collaboration, *The Angular Resolution of the Hegra Scintillation Counter Array at La Palma*, Ann Arbor 1990 Proceedings, High Energy Gamma-Ray Astronomy 127-131.

[3] Giglietto, N. *Performance of the MACRO detector at Gran Sasso: Moon shadow and seasonal variations*, 1997, Nuclear Physics B Proceedings Supplements, Volume 61, Issue 3, p. 180-184.

[4] M.O. Wasco for the Milagro collaboration, *Study of the Shadow of the Moon and the Sun with VHE Cosmic Rays*, 1999 arXiv:astro-ph/9906.388v1

[5] The Soudan 2 collaboration, *Observation of the Moon Shadow in Deep Underground Muon Flux*, 1999 arXiv:hep-ex/9905.044v1

[6] The Tibet AS Gamma Collaboration, M. Amenomori, *et al.* , *Multi-TeV Gamma-Ray Observation from the Crab Nebula Using the Tibet-III Air Shower Array Finely Tuned by the Cosmic-Ray Moon's Shadow*, arXiv:astro-ph/0810.3757v1

[7] L3 Collaboration, P. Achard *et al.* , *Measurement of the Shadowing of High-Energy Cosmic Rays by the Moon: A Search for TeV-Energy Antiprotons* Astropart.Phys.23:411-434,2005, arXiv:astro-ph/0503472v1

[8] D. Heck, J. Knapp, J.N. Capdevielle, G. Schatz, T. Thouw, *CORSIKA: A Monte Carlo Code to Simulate Extensive Air Showers*, FZKA 6019 (1998)

[9] Li, T.-P. and Ma, Y.Q., *Analysis methods for results in gamma-ray astronomy* 1983, ApJ 272,317